International Journal of Mass Spectrometry and Ion Processes, 75 (1987) 181–208
Elsevier Science Publishers B.V., Amsterdam – Printed in The Netherlands

INTERNAL ENERGY DISTRIBUTIONS OF ISOLATED IONS AFTER ACTIVATION BY VARIOUS METHODS

VICKI H. WYSOCKI, HILKKA I. KENTTÄMAA *† and R. GRAHAM COOKS *
Department of Chemistry, Purdue University, West Lafayette, IN 47907 (U.S.A.)
(First received 2 September 1986; in final form 19 December 1986)

ABSTRACT

A number of activation methods have been compared by approximating internal energy distributions, $P(E)$, of selected activated ions. The ions chosen allow simplifying assumptions to be made concerning the determination of the energy distributions since they fragment by several simple consecutive reactions. Ion abundance data, in combination with known energetics of unimolecular fragmentation, are utilized to estimate the internal energy distributions. Determination of $P(E)$ is therefore not based on a specialized instrument or technique and may be applied to ions which do not have stable neutral counterparts. The data obtained are used to account for several important features of tandem mass spectrometry and to examine and compare different methods of varying ion internal energy. The results show, inter alia, that (i) the general shapes of the energy distributions resulting from collisional activation are relatively insensitive to ion structure; (ii) the average energy of ions activated by collision in the kiloelectron volt or electron volt range of collision energy can be comparable; (iii) in contrast to low energy collisional activation, the distribution of internal energies produced by a kiloelectron volt collision is characterized by a finite probability of depositing very high energies; (iv) the average energy of fragmenting $(C_2H_5)_4Si^{+\cdot}$ ions appears to vary linearly with the collision energy in the 5–28 eV range. As the collision energy increases, the width of the internal energy distribution appears to broaden.

INTRODUCTION

The internal energy distribution of a population of ions exerts a controlling influence on its reactivity. The dependence of the unimolecular rate constant on ion internal energy lies at the heart of theories of mass spectra [1–4] and some elegant experiments [5–10] have addressed this relationship.

* To whom correspondence should be addressed.
† On leave from the Department of Chemistry, University of Helsinki, with a fellowship from the Academy of Finland.

0168-1176/87/$03.50

Furthermore, there are practical advantages to *controlling* ion internal energy in mass spectrometry. Systematic variation of the amount of energy present in fragmenting ions has proven to be useful, for example, in optimizing molecular ion abundances [11–16] and in isomer differentiation [15–18]. Unfortunately, few of the methods generally used to activate and dissociate gas-phase ions allow easy, well-defined control of ion internal energies over a wide range [19]. With the advent of tandem mass spectrometry as a tool in mixture analysis [20–22] and ion structural characterization [20,23,24], the number of methods used to activate ions has increased. These methods include collisions of fast ions with a stationary gas-phase target in the high-energy (kiloelectron volt) [20,25–29] and low-energy (electron volt) [20,30–33] ranges of laboratory ion kinetic energy, as well as photodissociation [34–37] and surface-induced dissociation [38,39]. Depending upon the choice of experimental conditions, the individual methods allow some measure of control over the degree of excitation of a selected ion. The techniques of angle-resolved mass spectrometry (ARMS) [20,24,40–42] and energy-resolved mass spectrometry (ERMS) utilizing collisional activation with gaseous targets [20,24,43–45] have proven to be especially useful in controlling the extent of activation.

These developments focus attention on a central issue in mass spectrometry, viz. what is the internal energy distribution of a particular population of isolated ions? In spite of extensive efforts, a great deal remains to be learned about the internal energy distributions, $P(E)$, of isolated ions [1,19]. Existing procedures used to characterize $P(E)$ include differentiation of ionization efficiency curves [46–50]. This method gives an estimate of $P(E)$ but is applicable only to ions generated by electron ionization or photoionization. Photoelectron-photoion coincidence spectroscopy [7,8,51,52] accurately defines the internal energy of ions, but it is an experimentally difficult technique and can only be applied to photoionization. Nevertheless, it has supplied definitive values on $P(E)$ distributions. It has been suggested that modification of photoelectron spectra yields information on $P(E)$ associated with electron ionization [1,10] and this approach has provided extremely valuable insights into unimolecular ion chemistry. There has also been an attempt [27] to modify $P(E)$ data obtained from photoelectron spectra according to the ratio of ion abundances in the electron ionization and collisional activation spectra to yield $P(E)$ for collisional activation. None of the above methods is applicable to ions which do not have stable neutral counterparts and such ions present some of the most interesting ion structural problems [53–59]. This limitation is avoided in approaches based on the probability of electronic excitation in high-energy collisions, as in studies in which transition probabilities were utilized to deduce $P(E)$ curves for ionized methane [60,61] and ionized toluene [60].

Since $P(E)$ has proven elusive, a number of workers have used a different approach to obtain information on the energies acquired by ions upon excitation. Comparison of the amounts of energy deposited using different activation methods has been made on the basis of the extent of dissociation of the activated ions. For example, the branching ratio of the fragmentation products m/z 29 and m/z 31 has been used as a measure of energy deposition in methanol molecular ions in high-energy collisions with different targets [62] and in high-energy collisions which lead to scattering through different angles [41,42,62–65]. Branching ratios have been used to characterize energy deposition associated with photodissociation [66–69], charge exchange [70,71], and low-energy collisional activation [71–75]. The shapes of $P(E)$, however, have not been reported, although the *average* energy of the activated ion population was estimated in some of these studies by comparison of the measured branching ratios with those obtained independently, for example by photodissociation [73,75].

As a result of the efforts cited, generalizations have emerged regarding $P(E)$ of ions activated by different methods. Charge transfer data taken over a range of collision energies combined with simple assumptions regarding the velocity dependence of the cross-section for deposition of different amounts of internal energy (the Massey adiabatic criterion) [76,77] led to the conclusion that kiloelectron volt collisions result in a smooth $P(E)$ with a low-energy maximum and a long tail to higher internal energies [60]. Qualitative comparisons of the degree of fragmentation following collisional activation vs. that obtained by electron ionization have provided [27] the information that the average energy deposited in collisional activation is often less than that supplied during 70 eV electron ionization. Using the same approach, it was concluded that a smaller amount of energy can be deposited in low-energy collisions than in high-energy collisions [75,78]. However, low-energy collisional activation is often very sensitive to the ion kinetic energy [20]. Indeed, some recent results suggest similar [24,45,78] or larger [71,73,79] average energy deposition upon low-energy collisional activation than in high-energy collisional activation of certain compounds, such as small phosphorus esters [45,79] and $C_3H_6O^+$ ions [24].

The need for information on internal energy distributions associated with activated ions prompted us to use a *simple, systematic* method to approximate and compare the distributions of internal energies of ion populations after activation by different means [80]. Using these data, this paper seeks to account for some important features of tandem mass spectrometry, such as the effects of various experimental parameters on collisional activation. In addition, different methods of varying ion internal energy are examined and compared.

EXPERIMENTAL

All data were derived from an average of at least five spectra. No corrections were made for possible metastable ion contributions. Samples were introduced into the mass spectrometers by direct insertion probes. Electron ionization mass spectra (EIMS) were recorded using a Finnigan triple quadrupole mass spectrometer [81] or a Finnigan 4000 mass spectrometer.

The low-energy collision-induced dissociation (CID) spectra were obtained with a Finnigan triple quadrupole instrument [81] using argon as the collision gas. Ions were generated by 70 eV electron ionization unless otherwise noted. Argon pressure was monitored with a Bayard–Alpert ionization gauge situated outside the closed collision chamber. The indicated pressure was less than 3×10^{-6} torr for single-collision conditions; a linear increase in fragment ion abundances as a function of target pressure was taken as a criterion for single-collision conditions [82]. For multiple-collision conditions, the argon pressure in the collision chamber was raised until the gauge pressure was about 5×10^{-5} torr (about 2 mtorr in the collision quadrupole). Under these conditions, ions which do not fragment during activation undergo roughly 15 collisions with argon atoms (estimated from the pressure limit of single-collision conditions). For charge exchange experiments, the ion source was operated in the CI mode and 70 eV electron ionization was used to ionize the charge exchange reagents (argon, xenon, and CS_2; recombination energies: 15.8, 12.2, and 10.1 eV, respectively) [83]. The nominal pressure of the reagent gas in the ion source was 0.2–0.3 torr.

High-energy collision-activated dissociation was performed with a reversed geometry instrument of the MIKES type [84]. Radical ions were generated by charge exchange using argon ions. The nominal ion source pressure was 0.3 torr. Air or argon was used as the collision gas at a pressure corresponding approximately to single-collision conditions (an indicated pressure of about 2×10^{-5} torr as measured with a Bayard–Alpert ionization gauge outside the collision chamber).

The compounds were obtained commercially and used without purification.

RESULTS

Estimation of internal energy distributions

Mass spectra are calculated knowing (i) the fragmentation reaction sequences of the ionized molecules, (ii) the energy-dependent unimolecular rate constants of each fragmentation reaction, (iii) the reaction time, and (iv)

the internal energy distribution, $P(E)$, of the ionized molecules [1]. In principle, it is possible to rearrange these parameters and to determine $P(E)$ from the mass spectrum [10,27,49] or, more generally, from the daughter ion spectrum of any selected ion [27,80]. The distribution $P(E)$ then refers to a population of ions which has been activated to cause dissociation. These ideas have been employed in several attempts to determine $P(E)$ on the basis of mass spectra [10,27,49,80].

Application of the above concept to ions which fragment via complicated mechanisms producing several products in a competitive fashion is difficult due to the complexity of the calculations required. Moreover, detailed breakdown curves [27] and reaction rate constants for each dissociation reaction are needed. The procedure may be facilitated significantly by choosing ions which allow simplifying assumptions to be made. Using this approach, parent ions whose major fragmentation pathway consists of *several consecutive reactions with known activation energies and similar entropy requirements* are desirable in the present study. It is assumed that all except the most obvious kinetic effects are negligible, viz. all the parent ions which have enough internal energy to dissociate do so and undergo the most endothermic reaction open to them [85].

The simple method of approximating $P(E)$ is illustrated using an ion P^+ fragmenting via the reaction sequence

$$P^+ \underset{E_0(1)}{\rightarrow} F_1^+ \underset{E_0(2)}{\rightarrow} F_2^+ \underset{E_0(3)}{\rightarrow} F_3^+$$

All parent ions, P^+, with energies between the activation energies for formation of F_1^+ and F_2^+ [$E_0(1)$ and $E_0(2)$, respectively] are assumed to fragment to yield F_1^+, whereas ions P^+ with internal energies between $E_0(2)$ and $E_0(3)$ will fragment to F_2^+, etc. The relative abundance of each fragment ion (F_n^+) is taken as a measure of the number of the ions P^+ with internal energies in the energy range where the formation of the fragment dominates. As an example, F_1^+ is the major product of those ions P^+ which have internal energies between $E_0(1)$ and $E_0(2)$, with an unweighted average energy of $[E_0(1) + E_0(2)]/2$. The abundance of F_1^+ divided by the energy range $E_0(2)-E_0(1)$ gives the data point of $P(E)$ at $[E_0(1) + E_0(2)]/2$. This procedure is followed for each fragment, thus mapping the shape of $P(E)$ (see Fig. 1). The number and intervals of the data points are set by the number of consecutive reactions and their activation energies. The larger the number of reactions and the smaller the difference between their activation energies, the more accurately the shape of $P(E)$ can be estimated. The method does not lend itself to determining fine structure which may be present in $P(E)$ distributions.

In the present study, appearance energies which were mainly determined by electron ionization [83,86–91] are used without correction. Energy parti-

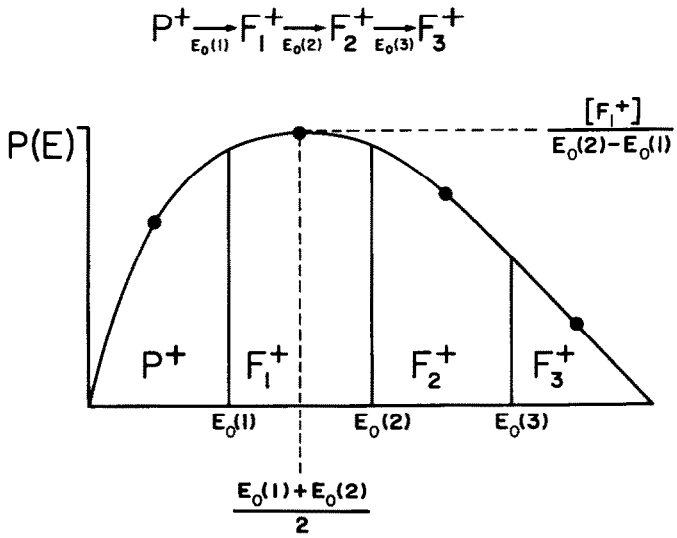

Fig. 1. Determination of internal energy distributions, $P(E)$, from ion abundances, $[F_i]$, and activation energies for fragmentation $E_0(i)$ (see the text). The curves are normalized to the highest datum point.

tioning between the neutral and the ionic fragments and the kinetic shift are taken into account by assuming that they are similar for electron ionization-induced dissociation and for fragmentation induced by the other methods studied. This is a rough approximation and may not hold in all instances; for example, energy partitioning may be different at the threshold for dissociation and far above the threshold. To minimize the problems caused by energy partitioning, parent ions which fragment by loss of small neutrals are used since small neutral fragments are not expected to carry much energy in their internal degrees of freedom. Instrumental discrimination effects as well as ion loss mechanisms, such as scattering and neutralization, are not considered. Metastable ions, which represent a small fraction of total ion abundance (typically less than 1%) are also neglected.

In contrast to many earlier attempts to characterize $P(E)$, which aimed to describe the energy deposition upon *formation* of the ions, what is measured here is the *final* internal energy distribution after ion formation and activation. As such, this approach is particularly appropriate for the estimation of energy deposition in tandem mass spectrometry and in other situations in which ions of low (sometimes negligible) internal energy are activated in order to cause dissociation. In such circumstances, interest in the final internal energy is tantamount to interest in the energy deposition upon activation.

Ions chosen for approximations of P(E)

Internal energy distributions were approximated for activated $Fe(CO)_5^{+\cdot}$, $W(CO)_6^{+\cdot}$, $Fe(CO)_4^{-\cdot}$, and $(C_2H_5)_4Si^{+\cdot}$ ions under different experimental conditions. These ions meet the requirements necessary for simple approximation of $P(E)$: each fragments via a single series of similar reactions with no significant competitive reactions (see, for example, the spectra in Fig. 3) and the activation energies for the fragmentation reactions are known (Table 1). The linear fragmentation pathways which dominate for ionized metal carbonyls are well established [92]. An organic ion which meets the above requirements is difficult to find. Tetraethylsilane was chosen although the entropy requirements of its reactions may differ more than desired. The similarity of the $P(E)$ of this ion to the $P(E)$ of other ions used (see data) suggests that the differences in the entropy requirements in this case are not a controlling factor in approximate determination of $P(E)$. Fragmentation of $(C_2H_5)_4Si^{+\cdot}$ follows a linear reaction sequence through formation of the ion of m/z 59, but competition occurs between formation of the ions of m/z 57 and m/z 31 from m/z 59 as energies above the threshold for formation of both these fragments are reached. Only the lower energy product, the ion of m/z 57, is considered in the calculations, even in the cases where competition occurs. The $P(E)$ distributions are not significantly affected by this omission since the ions of m/z 57 and m/z 31 are minor products under all forms of activation used.

Since all of the ions studied fragment by loss of small neutral fragments, the assumption that only a small amount of energy is carried away by the neutral fragment seems justified. A recent experimental (TPEPICO) breakdown curve for $Cr(CO)_6^{+\cdot}$ shows this to be a good assumption in the low internal energy range, although it is less valid at higher internal energies [52].

The validity of the approach used in this study is supported by comparison of the $P(E)$ obtained for electron ionization of $W(CO)_6$ with the corresponding photoelectron spectrum [93] (Fig. 2). There is a strong similarity between the photoelectron spectrum and the $P(E)$ obtained by our approach. From Fig. 2, it is apparent that the gross features of $P(E)$ are well described by the present method, although fine structure cannot be estimated.

P(E) data obtained

The results are presented in three separate sections. In the first section, $P(E)$ distributions of ions which have suffered a single high- or low-energy collision with an atomic gaseous target are compared. In the second section, $P(E)$ distributions obtained for ions excited (and, in some instances, also

TABLE 1

Thermochemical data

Ion	m/z	IE/AE [a]	E_0 [b]
$Fe(CO)_5^{+\cdot}$	196	8.0	0.0
$Fe(CO)_4^{+\cdot}$	168	9.1	1.1
$Fe(CO)_3^{+\cdot}$	140	10.1	2.1
$Fe(CO)_2^{+\cdot}$	112	11.3	3.3
$Fe(CO)^{+\cdot}$	84	13.5	5.5
$Fe^{+\cdot}$	56	15.5	7.5
$FeC^{+\cdot}$	68	23.6	15.6
$W(CO)_6^{+\cdot}$	352	8.5	0.0
$W(CO)_5^{+\cdot}$	324	9.7	1.2
$W(CO)_4^{+\cdot}$	296	11.9	3.4
$W(CO)_3^{+\cdot}$	268	13.7	5.2
$W(CO)_2^{+\cdot}$	240	16.0	7.5
$W(CO)^{+\cdot}$	212	18.6	10.1
$W^{+\cdot}$	184	21.5	13.0
$W(C_2O)^{+\cdot}$	224	25.9	17.4
$(C_2H_5)_4Si^{+\cdot}$	144	10.5	0.0
$(C_2H_5)_3Si^+$	115	11.0	0.5
$(C_2H_5)_2SiH^+$	87	12.5	2.0
$(C_2H_5)SiH_2^+$	59	14.0	3.5
$(C_2H_5)Si^+$	57	19.4	8.9
SiH_3^+	31	20.6	10.1
SiH^+	29	26.8	16.3
$Fe(CO)_4^{-\cdot}$	168	0.0	0.0
$Fe(CO)_3^{-\cdot}$	140	0.3	0.3
$Fe(CO)_2^{-\cdot}$	112	2.8	2.8
$Fe(CO)^{-\cdot}$	84	3.7	3.7
$Fe^{-\cdot}$	56	5.9	5.9

[a] The ionization energy (IE) for $Fe(CO)_5$ and the appearance energies (AE) for its fragments are average values based on refs. 86–89. The IE(AE) for $W(CO)_6$ and its fragments are average values based on refs. 87–89. The IE(AE) for $(C_2H_5)_4Si$ and its fragments are from ref. 90, except for the value for $(C_2H_5)SiH_2^+$ which was estimated based on the assumption that approximately the same amount of energy is needed to lose C_2H_4 from m/z 115 and m/z 87 (recent experimental data from our laboratory support this treatment). The data for $Fe(CO)_4^{-\cdot}$ and its fragments are from ref. 91.

[b] The activation energies for fragmentation, E_0, were obtained by taking the difference between the appearance energy, AE, for a given fragment and the ionization energy, IE, for the corresponding molecule.

generated) using a variety of other excitation methods are described. The final section focusses on the effects of ion source as well as collision region conditions on $P(E)$ of ions activated by low-energy collisional activation.

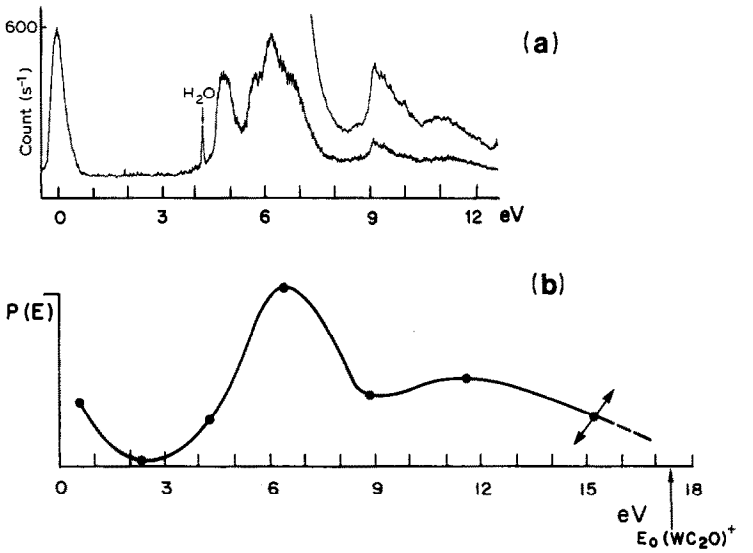

Fig. 2. Comparison of (a) the photoelectron spectrum of $W(CO)_6$ [93] and (b) the estimated $P(E)$ distribution for $W(CO)_6^{+\cdot}$ ions generated and activated by 70 eV electron ionization.

P(E) of ions activated by single high- or low-energy collisions with a gas-phase target

$P(E)$ distributions obtained for $Fe(CO)_5^{+\cdot}$ ions activated by a single collision with a stationary argon target at high (7 keV) or low (5 eV, 28 eV) laboratory ion kinetic energy are shown in Fig. 3. The collision-induced dissociation (daughter ion) spectra which were used to derive $P(E)$ are shown in the same figure. The maximum internal energies of the ions after collision is expected to be given by the sum of their center-of-mass kinetic energy, E_{cm}, and their maximum internal energy prior to collision, E_0 (which is assumed to be equal to the activation energy of the lowest energy fragmentation). These energies are indicated in Fig. 3(e) and (f) and they agree reasonably well with the experimentally observed values.

The $P(E)$ distributions obtained for $(C_2H_5)_4Si^{+\cdot}$ and $W(CO)_6^{+\cdot}$ activated by single low- and high-energy collisions are shown in Figs. 4 and 5, respectively. The expected maximum energies ($E_{cm} + E_0$) are in good agreement with the observed maxima for $(C_2H_5)_4Si^{+\cdot}$ (for 28 eV laboratory ion kinetic energy, the expected maximum energy is 6.6 eV, the observed is 6.3 eV), but not for $W(CO)_6^{+\cdot}$ (for 28 eV laboratory ion kinetic energy, the expected maximum energy is 4.1 eV, but the observed is about 6.5 eV). The most probable reason for the discrepancy between the expected and observed maximum energies of fragmenting $W(CO)_6^{+\cdot}$ ions is that the appearance energies used to estimate $P(E)$ for $W(CO)_6^{+\cdot}$ (see Table 1) are in

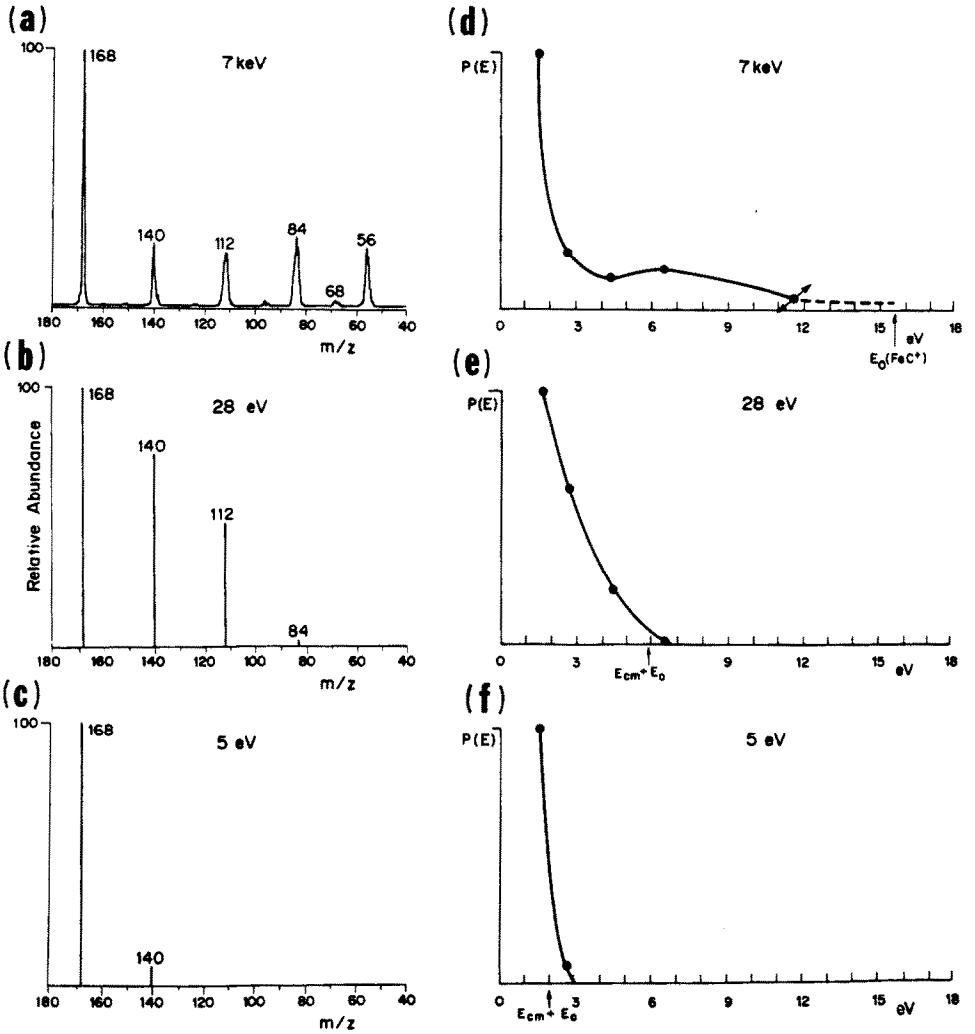

Fig. 3. Collision-induced dissociation (CID) spectra, (a)–(c), and the corresponding $P(E)$ distributions, (d)–(f), obtained for $Fe(CO)_5^{+\cdot}$ ions activated by a single collision with a gas-phase argon atom at 7 keV, 28, or 5 eV laboratory ion kinetic energy. The presence of the FeC^+ (m/z 68) ion for 7 keV CID indicates that the $P(E)$ distribution must extend to at least 15.65 eV and also directs placement of the point corresponding to $[Fe^{+\cdot}]$ midway between $E_0[Fe(CO)^{+\cdot}]$ and $E_0(FeC^{+\cdot})$. ↙ indicates uncertainty in the placement of a point on the curve.

error; there is a great variation in the appearance energies reported in the literature for this particular case [83]. Unfortunately, the correctness of the energy axis of the $P(E)$ distributions depends on the accuracy of the experimental method used to determine the appearance energies and these can be poor for reasons discussed extensively elsewhere [1,5,83].

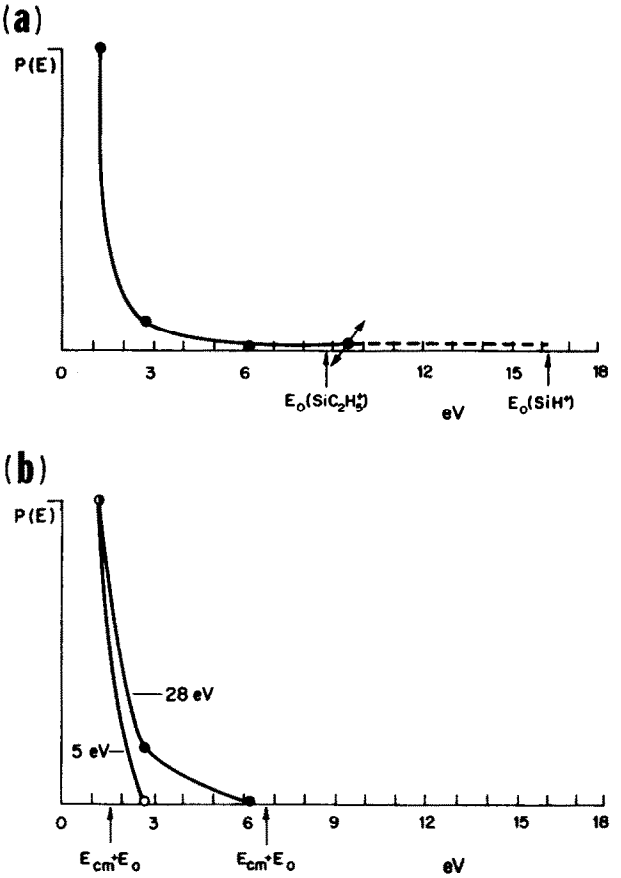

Fig. 4. $P(E)$ distributions obtained for $(C_2H_5)_4Si^{+\cdot}$ ions activated by a single collision with a gas-phase argon atom at (a) 7 keV and (b) 5 eV or 28 eV laboratory ion kinetic energies.

The maximum energy deposited in all the ions studied is found to be less than 4 eV in collisions with argon at 5 eV laboratory ion kinetic energy and less than 6 eV in collisions at 28 eV (as calculated by subtracting E_0 for the lowest energy dissociation process from the maximum energy indicated by the curves). The shapes of the $P(E)$ distributions obtained for low-energy collisional activation are remarkably similar, regardless of the ion used, and they also closely resemble those obtained for $(C_2H_5O)_3PO^{+\cdot}$ in a preliminary study [80]. The curves are smooth and show a single maximum. The general shapes of the distributions obtained for high-energy collisional activation are different from those of low-energy collisional activation, but are also relatively insensitive to the ion chosen. Unfortunately, the distribution of energies deposited in 5 eV, single-collision experiments cannot be

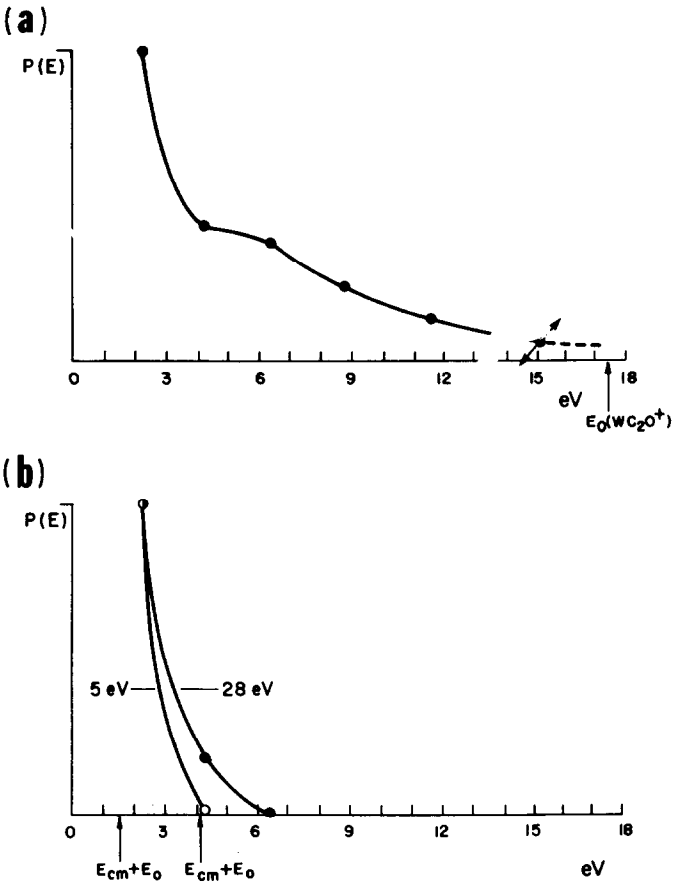

Fig. 5. $P(E)$ distributions obtained for $W(CO)_6^{+\cdot}$ ions activated by a single collision with a gas-phase argon atom at (a) 7 keV and (b) 5 eV or 28 eV laboratory ion kinetic energies.

well characterized for the ions studied since very little fragmentation is observed under these conditions. The abundance of the parent ion is not used in the determination of $P(E)$ associated with single-collision experiments since the percentage of parent ions which have undergone a collision without fragmenting is unknown. Therefore, the distributions presented for single-collision conditions (Figs. 3–5) refer only to *fragmenting* ions; as a result, no information is obtained on the probabilities of depositing energy in the energy range $E = 0$ to $E = E_0(1)$.

Quantitative estimates of energy deposition were made using data obtained for the $(C_2H_5)_4Si^{+\cdot}$ ions. The fragmentation threshold is only 0.5 eV for these ions and the average internal energy of the $(C_2H_5)_4Si^{+\cdot}$ ions prior to collisional excitation can therefore be assumed to be negligible. The

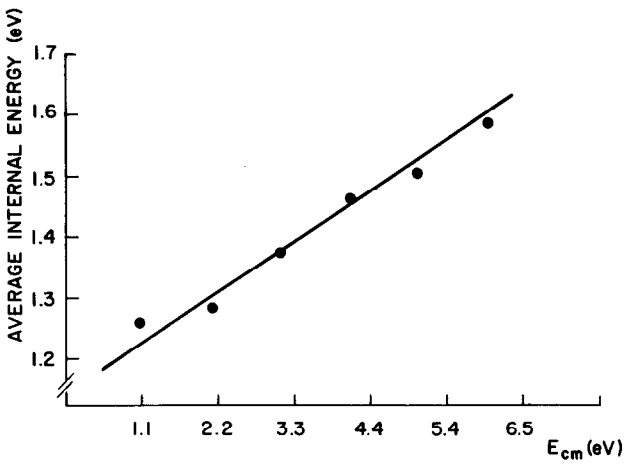

Fig. 6. The average energy of fragmenting $(C_2H_5)_4Si^{+\cdot}$ ions after a single low-energy gas-phase collision with argon is apparently a linear function of the ion kinetic energy in the range of 5–28 eV (plotted as center of mass energy, E_{cm}).

average energy of $(C_2H_5)_4Si^{+\cdot}$ ions which fragment after a single 28 eV or 7 keV collision was found to be 1.6 eV in both cases (obtained from the curves in Fig. 4 by weighting the distributions after setting $P(E) = 0$ for $E < [E_0(2) + E_0(1)]/2$). In the 5–28 eV collision energy range, the average energy appears to vary linearly with the ion kinetic energy (Fig. 6), although the quality of the data does not allow unambiguous determination of the power of the energy dependence. Similar results for other systems were obtained earlier in a comparison of branching ratios obtained by collisional activation and charge exchange [71] and in an experiment in which the inelasticity was directly measured [33]. At very low ion kinetic energies, the fraction of the theoretical maximum energy, E_{cm}, transferred into internal energy is high, but it levels off at higher collision energies. This result is in agreement with the suggestions of high transfer efficiency made earlier by other groups based on comparison of (i) threshold behavior with that expected on the basis of photoionization data [82] and (ii) branching ratios obtained by collisional activation with those obtained by charge exchange [71], photodissociation [73], and calculated breakdown curves [43].

P(E) of ions activated by other methods

Temperature effects on metastable ion abundances have been interpreted to indicate that complex $P(E)$ distributions having multiple maxima and minima are associated with *electron ionization* [10]. Photoelectron spectra, which are based on a vertical ionization process like electron ionization, support this conclusion [1,10]. It is of interest to check the present method

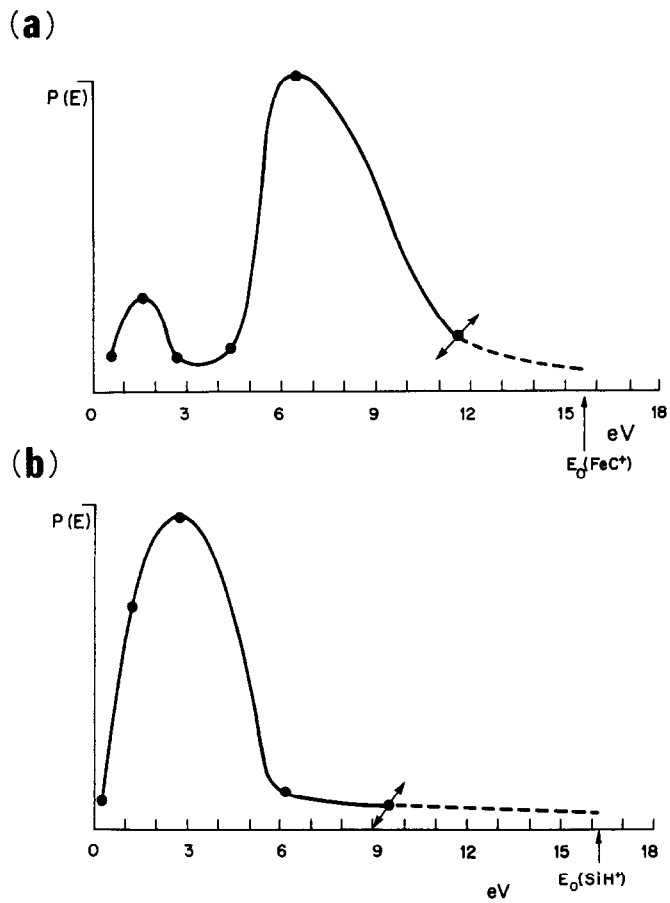

Fig. 7. $P(E)$ distributions obtained for (a) $Fe(CO)_5^{+\cdot}$ and (b) $(C_2H_5)_4Si^{+\cdot}$ ions generated and activated by 70 eV electron ionization.

against these results. If the shape of the $P(E)$ distribution for electron ionization is very different from the shapes observed for collisional activation, as the above reports suggest, similarities between electron ionization mass spectra and collision-activated dissociation spectra cannot be deep-seated. To address these questions, $P(E)$ distributions were estimated for $W(CO)_6^{+\cdot}$, $Fe(CO)_5^{+\cdot}$, and $(C_2H_5)_4Si^{+\cdot}$ ions generated (and activated) by electron ionization [Figs. 2(b) and 7]. In contrast to the curves obtained for collisional activation of the same set of ions (Figs. 3–5), all these curves have different shapes and two of them have at least two maxima. These results agree with the earlier findings and suggest that detailed comparisons of electron ionization and collision-induced dissociation spectra are by no means straightforward.

Charge exchange experiments are frequently used to vary ion internal energy in a systematic fashion [6,16,70,71]. The energy deposition in these experiments is assumed to be very well defined, in spite of the possibility of collisional deactivation of the ions after electron transfer. Figure 8 shows the $P(E)$ distributions obtained for $W(CO)_6^{+\cdot}$ generated and excited by charge exchange with argon and xenon reagent ions. The curve obtained using $Ar^{+\cdot}$ is very narrow indeed. The average energy deposited (6.4 eV) is close to the expected value (7.3 eV), which is simply the difference between the recombination energy of the reagent ion and the ionization potential of the neutral, $RE(Ar^{+\cdot}) - IE[W(CO)_6]$. This suggests that collisional relaxation does not present a serious problem in charge exchange of $W(CO)_6$, in spite of the relatively high pressures employed. It should be noted, however, that the example deals with an ion which fragments only by fast simple bond cleavages and that deactivation may be competitive with slower reactions, e.g. rearrangements, which dominate the fragmentation of some systems such as $(C_2H_5)_4Si^{+\cdot}$. Indeed, the $P(E)$ of $(C_2H_5)_4Si^{+\cdot}$ generated and activated by charge exchange with $Ar^{+\cdot}$ was found to be broad [about twice as wide as the curve obtained for $W(CO)_6^{+\cdot}$], which suggests that substantial collisional deactivation occurs in this case. In contrast, the triethylphosphate radical cation produced by charge exchange with $Ar^{+\cdot}$ fragments only to those ions (m/z 82, 99, 109) which are expected based on a narrow $P(E)$ centered near $RE(Ar^+) - IE[(C_2H_5O)_3PO]$. This ion fragments via rearrangement reactions [80] and collisional activation does not appear to be competitive with dissociation.

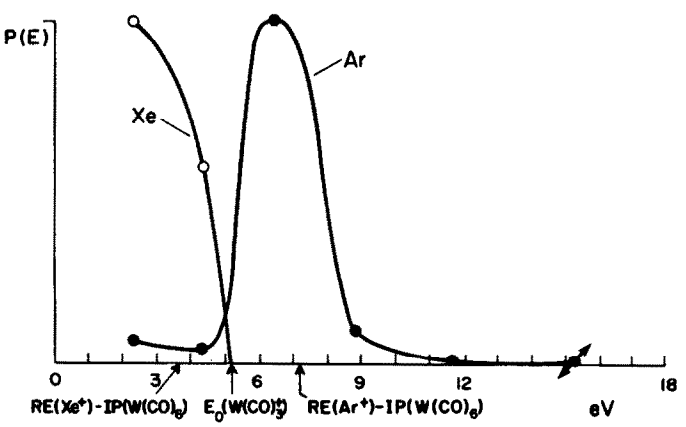

Fig. 8. $P(E)$ distributions obtained for $W(CO)_6^{+\cdot}$ ions generated and activated by charge exchange with xenon and argon ions.

Effects of ion source and collision region conditions on P(E) due to low-energy collisional activation

Low-energy collisional activation has proven to be especially sensitive to experimental conditions [20,31,32,45,79]. Therefore, it is of interest to examine how the $P(E)$ of ions activated by low-energy collision depends on some variables related to ion generation and excitation.

Figures 5(b) and 9 show $P(E)$ distributions obtained for $W(CO)_6^{+\cdot}$ ions generated by different methods prior to activation by a low-energy collision. Electron ionization [Fig. 5(b)] and charge exchange with reagent ions having different recombination energies ($CS_2^{+\cdot}$, $Ar^{+\cdot}$; Fig. 9) were used to ionize $W(CO)_6$ prior to low-energy collisional activation. No pronounced differences are seen in the $P(E)$ distributions obtained for the activated ions.

Effects of target pressure in low-energy collisional activation were studied using $Fe(CO)_5^{+\cdot}$, $W(CO)_6^{+\cdot}$, and $(C_2H_5)_4Si^{+\cdot}$ ions. When target pressure is

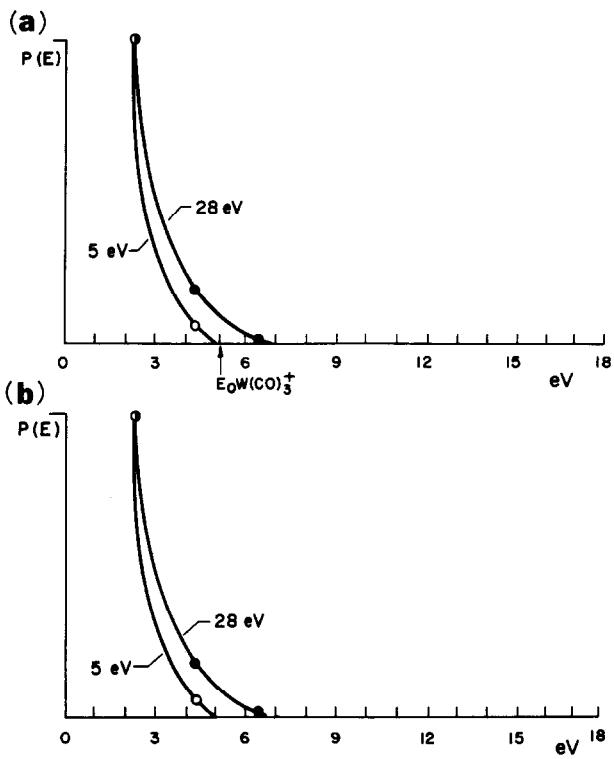

Fig. 9. $P(E)$ distributions obtained for $W(CO)_6^{+\cdot}$ ions generated by charge exchange with (a) $CS_2^{+\cdot}$ and (b) $Ar^{+\cdot}$ and activated by a single collision with a gas-phase argon atom at 5 or 28 eV laboratory ion kinetic energy.

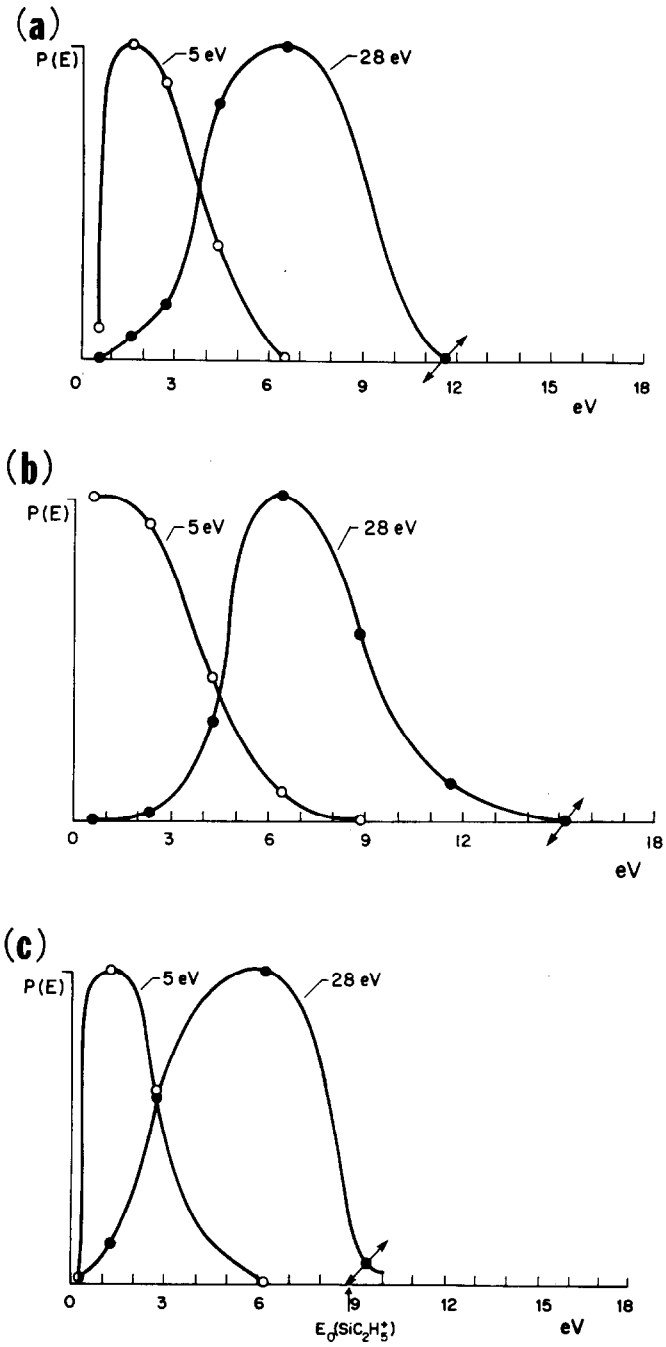

Fig. 10. Apparent $P(E)$ distributions obtained for (a) $Fe(CO)_5^{+\cdot}$, (b) $W(CO)_6^{+\cdot}$, and (c) $(C_2H_5)_4Si^{+\cdot}$ ions generated by electron ionization and activated using 5 or 28 eV laboratory ion kinetic energy and multiple-collision conditions (argon target).

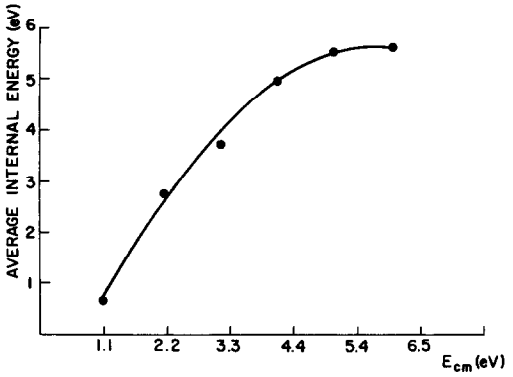

Fig. 11. The apparent average energy deposited by multiple gas-phase collisions increases rapidly with ion kinetic energy, accessing larger energies than are available in single-collision conditions (cf. Fig. 5).

high enough, a parent ion may undergo several activating collisions. Moreover, fragment ions may themselves be activated and dissociate [31,45,79, 94–96]. The results presented here are based on the final outcome of all these dissociation events and therefore differ fundamentally from those obtained using single-collision conditions. The $P(E)$ distributions shown for multiple-collision conditions (Fig. 10) indicate the *apparent* energy distribution which, if deposited in the *parent* ion in one activation step, would result in the same product ion distribution as is actually obtained under conditions in which both the parent ion and its fragment ions undergo collisions. These $P(E)$ distributions indicate that multiple activating collisions result in a significantly larger apparent average energy deposition than that obtained in a single collision (Figs. 3–5). This is the expected result based on earlier studies of pressure effects on low-energy CID spectra [1,32,94]. An average internal energy of ca. 5.6 eV would be needed to produce the same dissociation pattern from $(C_2H_5)_4Si^{+\cdot}$ ions activated in a single collision as is obtained for $(C_2H_5)_4Si^{+\cdot}$ ions with 28 eV initial kinetic energy under conditions where roughly 15 collisions take place between argon atoms and $(C_2H_5)_4Si^{+\cdot}$ ions and/or their fragments (Fig. 11). This amount of energy is about 3.5 times that obtained after a single 28 eV collision (1.6 eV; Fig. 6).

The apparent $P(E)$ distributions obtained for $Fe(CO)_4^{-\cdot}$ activated using multiple-collision conditions in *two different instruments*, a Fourier transform mass spectrometer (FTMS) [97,98] and a triple quadrupole instrument, are compared in Fig. 12. These curves are similar, in spite of the very different time scales of the two instruments and in spite of the unknown but probably wide range of collision energies associated with the FTMS experiment [74,97]. The negative ion $P(E)$ distributions (Fig. 12) are relatively

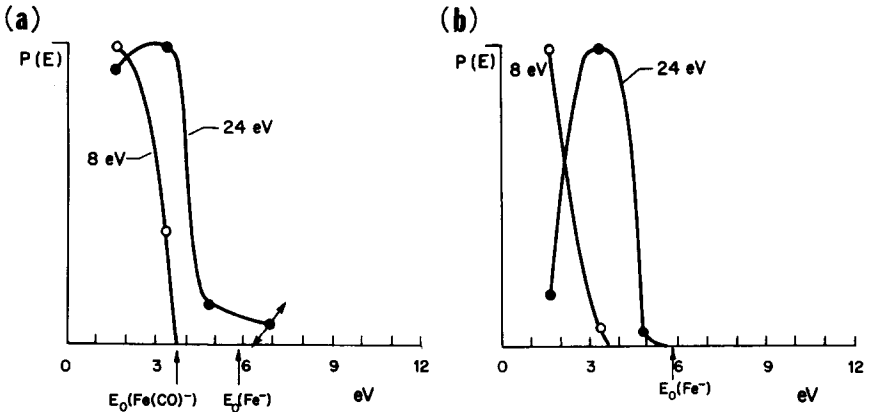

Fig. 12. Apparent $P(E)$ distributions obtained for $Fe(CO)_4^{-\cdot}$ activated under low-energy multiple-collision conditions (argon target) in (a) a Fourier Transform mass spectrometer (FTMS) at 10^{-5} torr and (b) a triple quadrupole mass spectrometer at about 2 mtorr. The $Fe(CO)_4^{-\cdot}$ ion abundance was not used in the determination of $P(E)$. Ion abundances for $P(E)$ approximation associated with the Fourier Transform mass spectrometer were obtained from ref. 98.

narrow in comparison with those obtained for positive ions (Fig. 10). This narrowness suggests that collision-induced electron detachment may be competing with collision-induced dissociation of the negative ions. Note that, although $Fe(CO)_4^{-\cdot}$ does not have a stable neutral counterpart, its $P(E)$ distribution can be estimated.

DISCUSSION

General characteristics of P(E) associated with different activation methods

The internal energy distributions presented in the previous section show the following characteristics. (i) In low-energy collisional activation, $P(E)$ shifts to higher energies with increasing collision energy, as expected [24,43,45,71,75,82]. However, as the collision energy increases, the width of the distribution appears to broaden, which is a drawback. (ii) Internal energy deposition can be increased in low-energy collisional activation by increasing target pressure. (iii) Significantly higher *total* energy deposition is available in high-pressure, low-energy collisional activation than in low-energy collisional activation under single-collision conditions. However, notice that the way in which the energy is deposited is different for these experiments. (iv) The $P(E)$ distribution obtained for high-energy collisional activation has a low probability, high-energy tail which is absent for low-en-

ergy collisional activation. This result is in accordance with an electronic excitation mechanism for high-energy collisional activation [60,76,77], as expected. (v) The *average* internal energy of ions excited under single-collision conditions can be comparable for high- and low-energy collisions, depending on the collision energy used in the low-energy experiment. (vi) The average amount of energy present in ions generated by 70 eV electron ionization is higher than that observed for ions which have suffered either a high- or a low-energy collision. (vii) The apparent amount of energy deposited by multiple collisions in a Fourier Transform ICR spectrometer can be comparable with that obtained by multiple collisions in a triple quadrupole mass spectrometer. (viii) $P(E)$ distributions obtained for ions generated and activated by charge exchange can be narrow, but are not necessarily so. In this experiment, energy is deposited within a moveable envelope whose position and width are dependent on the recombination energy of the reagent ion used and on the relative rates of dissociation and collisional relaxation of the activated ions.

The results described above rationalize a number of earlier experimental findings. For example, it has been found that breakdown graphs obtained by varying the ion kinetic energy in collisional activation employing eV collisions do not always show much change at higher collision energies (above 30 eV) [24,43,74,99]. This can be explained by the finding that variation of ion kinetic energy causes only a small relative change in $P(E)$, mainly broadening the $P(E)$ curve. Therefore, significant changes in CID product distributions as a function of kinetic energy are expected only if the ion studied does *not* have a dominant low-energy reaction pathway. The low-probability, high-energy tail obtained for high-energy collisional activation, but not for low-energy collisional activation, is at least part of the reason why processes of high endothermicity, such as charge stripping and charge inversion, are commonly seen in collisional activation at high kinetic energies (keV) but not the electron volt regime [20].

A comparison of $P(E)$ distributions obtained using different methods to vary ion internal energy shows that, in the case of ions which fragment by fast reactions, $P(E)$ associated with charge exchange can be significantly narrower than that associated with the other activation methods (variation of ion kinetic energy or target pressure in low-energy collisional activation). The drawbacks of the charge exchange method are that the internal energy deposited in the ions can not be varied continuously, since it depends on the recombination energy of the reagent ion used, that only ions which have stable neutral counterparts can be studied [16], and that collisional deactivation may occur for those ions which fragment by slow reactions. A promising method for varying ion internal energy is offered by a recently introduced activation method, surface-induced dissociation [38,39], which is

applicable to ions generated by various methods. Moreover, preliminary results [100] suggest that the ions which fragment after collision with a surface have a narrow distribution of energies and that higher average energies can be accessed than by any other collisional activation method.

It was confirmed that total energy deposition can be significantly increased by increasing target pressure in low-energy collisional activation. This is *not* meant to suggest that multiple-collision and single-collision conditions are different only in the *amounts* of energy deposited. Use of multiple activating collisions, which involves stepwise energy deposition, may lead to serious complications in attempting to characterize ion structure since (i) both parent ions and fragment ions may undergo collisions and (ii) activated ions may isomerize between collisions. Indeed, this has been demonstrated in recent publications [45,79]. For ion structural characterization, single-collision conditions should be used. However, high target pressures may be analytically useful in those cases where only a few structurally characteristic fragments are observed under single-collision conditions.

It must be stressed that similar internal energy distributions of ions activated using different methods do not necessarily result in similar product distributions. In particular, effects of different time scales must always be taken into account. In cases where only small energy barriers separate isomeric ion structures or where the lowest energy reactions are relatively slow, activation methods and/or instruments having different time scales may produce remarkably different dissociation patterns, in spite of similar energy depositions.

Effects of differences in P(E) on fragmentation patterns

Ionized polynuclear aromatic hydrocarbons are known to produce numerous ionic dissociation products upon a high-energy collision but yield only a few fragments upon a low-energy collision [78]. On the other hand, some small organophosphorus compounds produce nearly identical fragmentation patterns when these two activation methods are used [45,79]. The observation of different extents of fragmentation upon high- vs. low-energy collision for some compounds, but not for others, can be explained using typical shapes of the $P(E)$ distributions associated with these methods of activation.

Figure 13(a) and (b) show typical shapes of $P(E)$ distributions of ions after a high- or a low-energy collision, respectively, together with the approximate activation energies of some fragmentation reactions of ionized phenanthrene. The activation energies are obtained by taking the difference between the appearance energy of each fragment and the ionization potential of phenanthrene [83]. It is seen that low-energy collisional activation

cannot deposit energies large enough for most of these reactions to occur. Accordingly, only those fragmentation products with the lowest energy requirements are observed in the low-energy daughter ion spectrum of the phenanthrene molecular ion [Fig. 13(d)]. In contrast, high-energy collisional activation has a low but finite probability of depositing high internal energies. Therefore, while most of the phenanthrene ions activated by a high-energy collision do not have enough energy to fragment, some of them acquire very high internal energies. The daughter ion spectrum recorded [Fig. 13(c)] is a result of fragmentation of these high-energy parent ions. Thus, the reasons for the dramatically different spectra obtained for ionized phenanthrene upon low- and high-energy collisional activation are the high activation energies of the major fragmentation reactions and the absence of a high-energy tail in the internal energy distribution associated with low-energy collisional activation.

In contrast to phenanthrene, ionized dimethyl phosphonate fragments mainly by low-energy pathways [45,83], as indicated by the activation

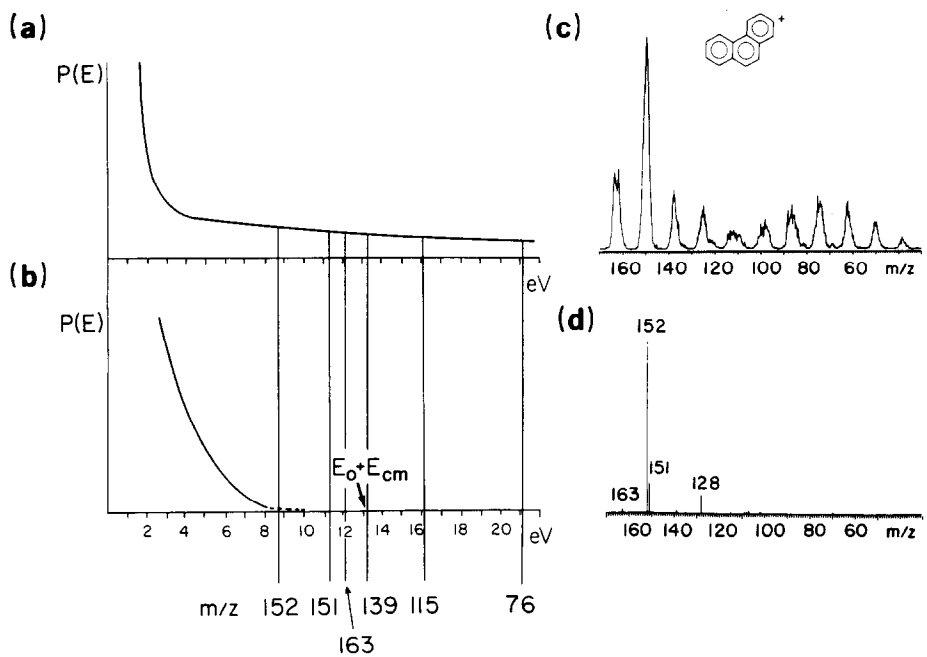

Fig. 13. Typical $P(E)$ distributions for ions after (a) high-energy (7 keV) or (b) low-energy (28 eV) collision with a gas-phase argon atom, and collision-induced dissociation daughter spectra of phenanthrene ions at (c) 7 keV and (d) 28 eV laboratory ion kinetic energies (argon target). Activation energies for various fragmentation products of phenanthrene, e.g. m/z 152, 151, 163, etc., are indicated by vertical lines on the $P(E)$ curves.

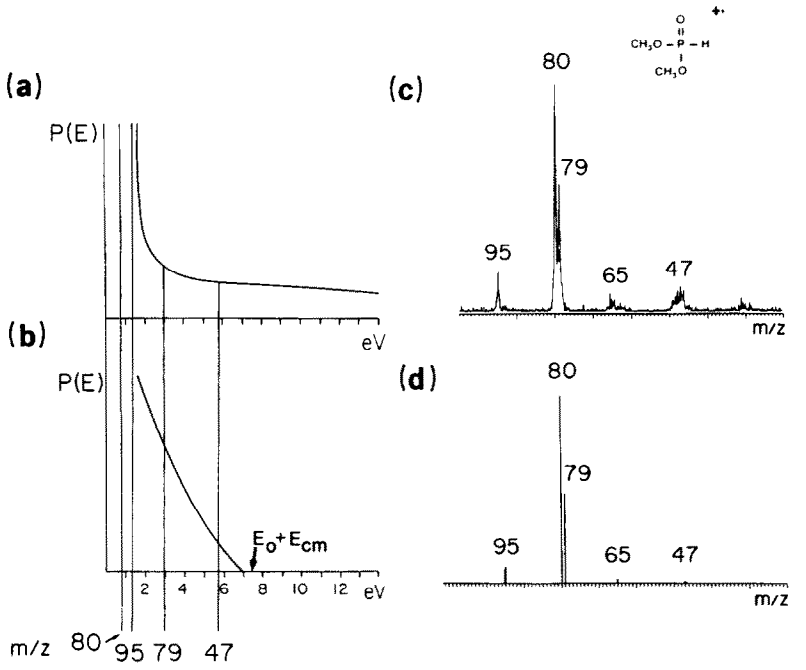

Fig. 14. Typical $P(E)$ distributions for ions after single (a) high-energy (7 keV) or (b) low-energy (25 eV) collisions with argon and collision-induced dissociation daughter spectra of dimethyl phosphonate ions at (c) 7 keV and (d) 25 eV laboratory ion kinetic energies (argon target). Activation energies for various fragmentation products of dimethyl phosphonate, e.g. m/z 80, 95, etc., are indicated by vertical lines on the typical $P(E)$ curves.

energies shown in Fig. 14(a) and (b). Differences in the internal energies deposited by high- and low-energy collisional activation are not large in the low internal energy range of $P(E)$ and hence the spectra obtained for ionized dimethyl phosphonate ions by these methods show only minor differences [Fig. 14(c), (d)].

Spectra obtained for the $(C_2H_5O)_3C^+$ ion (m/z 147) activated by various methods (Fig. 15) further demonstrate the control of $P(E)$ over fragmentation patterns. The average energy required to produce the major fragments

$$m/z\ 192 \xrightarrow{-45} m/z\ 147 \xrightarrow{-28} m/z\ 119 \xrightarrow{-28} m/z\ 91 \xrightarrow{-28} m/z\ 63 \xrightarrow{-18} m/z\ 45$$

presumably increases as more neutral molecules are eliminated, viz. in the order m/z 119 < m/z 91 < m/z 63 < m/z 45. The spectra indicate that much larger average energy deposition is achieved upon multiple low-energy collisions [Fig. 15(b), major peak at m/z 63] and upon electron ionization [Fig. 15(d), major peak at m/z 63] than in a single high- or low-energy

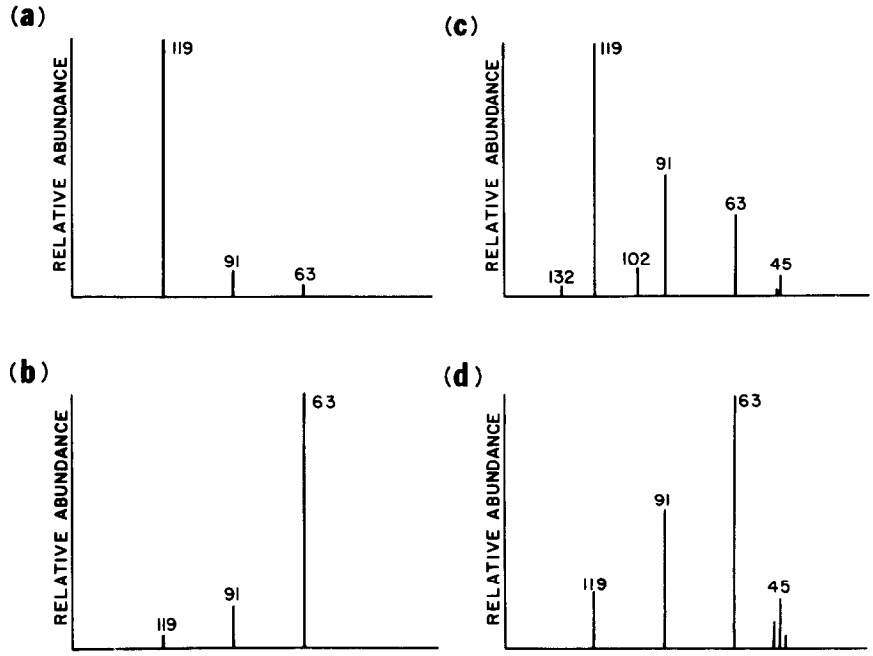

Fig. 15. Collision-induced dissociation daughter spectra of $(C_2H_5O)_3C^+$ ions (a) activated by a single gas-phase collision at 28 eV ion kinetic energy, (b) activated using 28 eV ion kinetic energy and multiple collision conditions, and (c) activated by a single gas-phase collision at 7 keV ion kinetic energy. (d) 70 eV electron ionization mass spectrum of $(C_2H_5O)_4C$ [the molecular ion $(C_2H_5O)_4C^{+\cdot}$ is not stable under these conditions and fragments to $(C_2H_5O)_3C^+$]. The $(C_2H_5O)_3C^+$ ion (m/z 147) is omitted from all the spectra to facilitate comparison.

collision [Fig. 15(a) and (c), major peak at m/z 119], in agreement with expectations based on the typical shapes of $P(E)$. The electron ionization mass spectrum of $(C_2H_5O)_4C$ [Fig. 15(d)] is similar to that obtained for $(C_2H_5O)_3C^+$ using 28 eV collision-induced dissociation under multiple-collision conditions [Fig. 15(b)]. In contrast, the electron ionization mass spectrum and the spectra obtained using a single activating collision are quite different, in agreement with $P(E)$ distributions for these activation methods.

An interesting aspect of the data in Fig. 15 is the formation of two high-mass, odd-electron products (m/z 102 and m/z 132) upon high-energy collisional activation. The corresponding peaks do not appear in any of the other spectra. The ions are therefore probably due to the high-energy, low probability tail of the $P(E)$ distribution associated with the high-energy collision experiment. It is concluded that the activation energies of the reactions forming the ions of m/z 102 and m/z 132 must be very high.

These reactions correspond to loss of an ethoxy radical or a methyl radical, respectively, from the $(C_2H_5O)_3C^+$ ion. In each of these reactions, two odd-electron products are formed from an even-electron ion, a process which contravenes the even-electron rule [1,11] and normally requires a large amount of energy.

CONCLUSIONS

Typical shapes of internal energy distributions and their relative positions on the energy axis were determined for isolated ions activated by different means. Information about the average internal energies of the ions was also obtained. However, the quantitative results should be considered as directive only, since the accuracy of this information is directly related to the correctness of the literature values of the appearance energies used to estimate $P(E)$ and because of several simplifying assumptions made in the treatment.

The great diversity of shapes of $P(E)$ demonstrates that a general knowledge of internal energy distributions of activated ions is of tremendous practical importance, especially in tandem mass spectrometry where various activation methods are used to dissociate ions. The data described in this paper rationalize a number of experimental findings, such as the sensitivity of low-energy collisional activation towards collision energy and target pressure. Results such as the limited sensitivity of $P(E)$ associated with collisional activation towards ion structure will be of importance in choosing the most suitable activation method for a particular ion type, as well as in the interpretation and comparison of results obtained for different ions or under different experimental conditions.

ACKNOWLEDGEMENTS

This work was supported by the National Science Foundation (CHE-8408258). H.I.K. acknowledges the support of the Academy of Finland.

REFERENCES

1 K. Levsen, Fundamental Aspects of Organic Mass Spectrometry, Verlag Chemie, Weinheim, New York, 1978.
2 A.G. Brenton, R.P. Morgan and J.H. Beynon, Ann. Rev. Phys. Chem., 30 (1979) 51.
3 H.M. Rosenstock, M.B. Wallenstein, A.L. Wahrhaftig and H. Eyring, Proc. Natl. Acad. Sci. U.S.A., 38 (1952) 667.
4 R.A. Marcus and O.K. Rice, J. Phys. Colloid Chem., 55 (1951) 894.
5 W.A. Chupka, J. Chem. Phys., 30 (1959) 191.
6 B. Andlauer and Ch. Ottinger, J. Chem. Phys., 55 (1971) 1471.

7 B. Brehm and E. von Puttkamer, Z. Naturforsch. Teil A, 22 (1967) 8.
8 T. Baer, in M.T. Bowers (Ed.), Gas Phase Ion Chemistry, Academic Press, New York, 1979, Vol. 1.
9 J.H.D. Eland, in R.A.W. Johnstone (Senior Reporter), Mass Spectrometry, Specialist Periodical Report, Vol. 5, The Chemical Society, London, 1979, Chap. 3.
10 F.W. McLafferty, T. Wachs, C. Lifshitz, G. Innorta and P. Irving, J. Am. Chem. Soc., 92 (1970) 6867.
11 H. Budzikiewicz, C. Djerassi and D.H. Williams, Mass Spectrometry of Organic Compounds, Holden-Day, San Francisco, 1967.
12 G. Spiteller and M. Spiteller-Friedmann, Liebigs Ann. Chem., 690 (1966) 1.
13 D.P. Stevenson and C.D. Wagner, J. Am. Chem. Soc., 72 (1950) 5612.
14 F.H. Field and S.H. Hasting, Anal. Chem., 28 (1956) 1248.
15 A.G. Harrison, Chemical Ionization Mass Spectrometry, CRC Press, Boca Raton, FL, 1983.
16 E. Lindholm, in J.L. Franklin (Ed.), Ion Molecule Reactions, Plenum Press, New York, 1972; pp. 457–484.
17 J. Sunner and I. Szabo, Int. J. Mass Spectrom. Ion Phys., 25 (1977) 241, 263.
18 A.N.H. Yeo and D.H. Williams, J. Am. Chem. Soc., 93 (1971) 395.
19 K.R. Jennings, Gazz. Chim. Ital., 114 (1984) 313.
20 F.W. McLafferty (Ed.), Tandem Mass Spectrometry, Wiley, New York, 1983.
21 R.G. Cooks and R.A. Roush, Chim. Ind. (Milan), 66 (1984) 539.
22 G.L. Glish, V.M. Shaddock, K. Harmon and R.G. Cooks, Anal. Chem., 52 (1980) 165.
23 K. Levsen and H. Schwarz, Angew. Chem. Int. Ed. Engl., 15 (1976) 509.
24 S. Verma, J.D. Ciupek and R.G. Cooks, Int. J. Mass Spectrom. Ion Processes, 62 (1984) 219.
25 K.R. Jennings, Int. J. Mass Spectrom. Ion Phys., 1 (1968) 227.
26 W.F. Haddon and F.W. McLafferty, J. Am. Chem. Soc., 90 (1968) 4745.
27 F.W. McLafferty, P.F. Bente III, R. Kornfeld, S.-C. Tsai and I. Howe, J. Am. Chem. Soc., 95 (1973) 2120.
28 R.G. Cooks (Ed.), Collision Spectroscopy; Plenum Press, New York, 1978.
29 K. Levsen and H. Schwarz, Mass Spectrom. Rev., 2 (1983) 77.
30 F. Kaplan, J. Am. Chem. Soc., 90 (1968) 4483.
31 R.A. Yost and C.G. Enke, Anal. Chem., 51 (1979) 1251A.
32 P.H. Dawson, J.B. French, J.A. Buckley, D.J. Douglas and D. Simmons, Org. Mass Spectrom., 17 (1982) 205, 212.
33 Z. Herman, J.H. Futrell and B. Friedrich, Int. J. Mass Spectrom. Ion Processes, 58 (1984) 181.
34 R.C. Dunbar, in M.T. Bowers (Ed.), Gas Phase Ion Chemistry, Vol. 2, Academic Press, New York, 1979, Chap. 14.
35 D.S. Bomse, R.L. Woodin and J.L. Beauchamp, J. Am. Chem. Soc., 101 (1979) 5503.
36 R.C. Dunbar, in M.T. Bowers (Ed.), Gas Phase Ion Chemistry, Vol. 3, Academic Press, New York, 1984, Chap. 20.
37 F.M. Harris and J.H. Beynon, in M.T. Bowers (Ed.), Gas Phase Ion Chemistry, Vol. 3, Academic Press, New York, 1984, Chap. 19.
38 Md.A. Mabud, M.J. DeKrey and R.G. Cooks, Int. J. Mass. Spectrom. Ion Processes, 67 (1985) 285.
39 M.J. DeKrey, Md. A. Mabud, R.G. Cooks and J.E.P. Syka, Int. J. Mass Spectrom. Ion Processes, 67 (1985) 295.
40 J.A. Laramee, J.J. Carmody and R.G. Cooks, Int. J. Mass Spectrom. Ion Phys., 31 (1979) 333.

41 D.M. Fedor and R.G. Cooks, Anal. Chem., 52 (1980) 679.
42 S. Verma, J.D. Ciupek, R.G. Cooks, A.E. Schoen and P. Dobberstein, Int. J. Mass Spectrom. Ion Phys., 52 (1983) 311.
43 D.D. Fetterolf and R.A. Yost, Int. J. Mass Spectrom. Ion Phys., 44 (1982) 37.
44 S.A. McLuckey, G.L. Glish and R.G. Cooks, Int. J. Mass Spectrom. Ion Phys., 39 (1981) 219.
45 H.I. Kenttämaa and R.G. Cooks, J. Am. Chem. Soc., 107 (1985) 1881.
46 R.W. Kiser, Introduction to Mass Spectrometry, Prentice Hall, Englewood Cliffs, NJ, 1965.
47 J.D. Morrison, J. Appl. Phys., 28 (1957) 1409.
48 W.A. Chupka and J. Berkowitz, J. Chem. Phys., 47 (1967) 2921.
49 H. Ehrhardt, F. Linder and T. Tekaat, Adv. Mass Spectrom., 4 (1968) 705.
50 W.A. Chupka and M. Kaminsky, J. Chem. Phys., 35 (1961) 1991.
51 M.M. Green, R.J. McCluskey and J. Vogt, J. Am. Chem. Soc., 104 (1982) 2262.
52 P.R. Das, T. Nishimura and G.G. Meisels, J. Phys. Chem., 89 (1985) 2808.
53 W.J. Bouma, J.K. MacLeod and L. Radom, J. Am. Chem. Soc., 104 (1982) 2930.
54 J.L. Holmes, F.P. Lossing, J.K. Terlouw and P.C. Burgers, J. Am. Chem. Soc., 104 (1982) 2931.
55 J.L. Holmes, F.P. Lossing, J.K. Terlouw and P.C. Burgers, Can. J. Chem., 61 (1983) 2305.
56 H. Halim, B. Ciommer and H. Schwarz, Angew. Chem. Int. Ed. Engl., 21 (1982) 528.
57 Y. Apeloig, B. Ciommer, G. Frenking, M. Karni, A. Mandelbaum, H. Schwarz and A. Weisz, J. Am. Chem. Soc., 105 (1983) 2186.
58 L. Radom, W.J. Bouma, R.H. Nobes and B.F. Yates, Pure Appl. Chem., 56 (1984) 1831.
59 E. Weger, K. Levsen, I. Ruppert, P.C. Burgers and J.K. Terlouw, Org. Mass Spectrom., 18 (1983) 327.
60 M.S. Kim and F.W. McLafferty, J. Am. Chem. Soc., 100 (1978) 3279.
61 M. Rabrenović, J.H. Beynon, S.H. Lee and M.S. Kim, Int. J. Mass Spectrom. Ion Processes, 65 (1985) 197.
62 P.H. Hemberger, J.A. Laramee, A.R. Hubik and R.G. Cooks, J. Phys. Chem., 85 (1981) 2335.
63 A.R. Hubik, P.A. Hemberger, J.A. Laramee and R.G. Cooks, J. Am. Chem. Soc., 102 (1980) 3997.
64 J.A. Laramee, P.H. Hemberger and R.G. Cooks, Int. J. Mass Spectrom. Ion Phys., 33 (1980) 231.
65 K.R. Jennings, R.S. Mason, M. Farncombe and R.G. Cooks, Int. J. Mass Spectrom. Ion Phys., 43 (1982) 327.
66 I.W. Griffiths, E.S. Mukhtar, R.E. March, F.M. Harris and J.H. Beynon, Int. J. Mass Spectrom. Ion Phys., 39 (1981) 125.
67 E.S. Mukhtar, I.W. Griffiths, F.M. Harris and J.H. Beynon, Int. J. Mass Spectrom. Ion Phys., 37 (1981) 159.
68 I.W. Griffiths, E.S. Mukhtar, F.M. Harris and J.H. Beynon, Int. J. Mass Spectrom. Ion Phys., 43 (1982) 283.
69 J.H. Chen, J.D. Hays and R.C. Dunbar, J. Phys. Chem., 88 (1984) 4759.
70 A.G. Harrison and M.S. Lin, Int. J. Mass Spectrom. Ion Phys., 51 (1983) 353.
71 S. Nacson and A.G. Harrison, Int. J. Mass Spectrom. Ion Processes, 63 (1985) 325.
72 G.L. Glish, S.A. McLuckey, T.Y. Ridley and R.G. Cooks, Int. J. Mass Spectrom. Ion Phys., 41 (1982) 157.
73 P.H. Dawson and W.-F. Sun, Int. J. Mass Spectrom. Ion Phys., 44 (1982) 51.

74 S.A. McLuckey, L. Sallans, R.B. Cody, R.C. Burnier, S. Verma, B.S. Freiser and R.G. Cooks, Int. J. Mass Spectrom. Ion Phys., 44 (1982) 215.
75 S.A. McLuckey, C.E.D. Ouwerkerk, A.J.H. Boerboom and P.G. Kistemaker, Int. J. Mass Spectrom. Ion Processes, 59 (1984) 85.
76 H.S.W. Massey, Rep. Prog. Phys., 12 (1949) 248.
77 J.B. Hasted, Physics of Atomic Collisions, Butterworths, London, 1964, Chap. 12.
78 J.D. Ciupek, D. Zakett, R.G. Cooks and K.V. Wood, Anal. Chem., 54 (1982) 2215.
79 H.I. Kenttämaa, Org. Mass. Spectrom., 20 (1985) 703.
80 For a preliminary communication, see H.I. Kenttämaa and R.G. Cooks, Int. J. Mass Spectrom. Ion Processes, 64 (1985) 79.
81 J.R.B. Slayback and M.S. Story, Ind. Res. Dev., Feb. (1981) 129.
82 J.A. Nystrom, M.M. Bursey and J.R. Hass, Int. J. Mass Spectrom. Ion Processes, 55 (1984) 263.
83 H.M. Rosenstock, K. Draxl, B.W. Steiner and J.T. Herron, J. Phys. Chem. Ref. Data, 6 Suppl. 1 (1977).
84 J.H. Beynon, R.G. Cooks, J.W. Amy, W.E. Baitinger and T.Y. Ridley, Anal. Chem., 45 (1973) 1023A.
85 This assumption has been used in procedures to estimate organic mass spectra, notably by Williams and co-workers: see R.G. Cooks, I. Howe and D.H. Williams, Org. Mass Spectrom., 2 (1969) 137.
86 R.E. Winters and R.W. Kiser, Inorg. Chem., 3 (1964) 699.
87 G.A. Junk and H.J. Svec, Z. Naturforsch. Teil B, 23 (1968) 1.
88 D.R. Bidinosti and N.S. McIntyre, Can. J. Chem., 45 (1967) 641.
89 A. Foffani and S. Pignataro, Z. Phys. Chem. (Frankfurt am Main), 45 (1965) 79.
90 J.J. de Ridder and G. Dijkstra, Rec. Trav. Chim., 86 (1967) 737.
91 R.N. Compton and J.A.D. Stockdale, Int. J. Mass Spectrom. Ion Phys., 22 (1976) 47.
92 M.R. Litzow and T.R. Spalding, Mass Spectrometry of Inorganic and Organo-Metallic Compounds, Elsevier, Amsterdam, 1973, pp. 475–490 and references therein.
93 D.W. Turner, C. Baker, A.D. Baker and C.R. Brundle, Molecular Photoelectron Spectroscopy, Interscience, New York, 1969, Chap. 14.
94 P.H. Dawson, Int. J. Mass Spectrom. Ion Phys., 43 (1982) 195.
95 M.S. Kim, Int. J. Mass Spectrom. Ion Phys., 50 (1983) 189.
96 C.E.D. Ouwerkerk, S.A. McLuckey, P.G. Kistemaker and A.J.H. Boerboom, Int. J. Mass Spectrom. Ion Processes, 56 (1984) 11.
97 R.B. Cody, R.C. Burnier and B.S. Freiser, Anal. Chem., 54 (1982) 96.
98 Ion abundances for $P(E)$ approximation: L. Sallens, K.R. Lane, R.R. Squires and B.S. Freiser, J. Am. Chem. Soc., 107 (1985) 4379.
99 J.J. Zwinselman, S. Nacson and A.G. Harrison, Int. J. Mass Spectrom. Ion Processes, 67 (1985) 93.
100 M.J. DeKrey, H.I. Kenttämaa, V.H. Wysocki and R.G. Cooks, Org. Mass. Spectrom., 21 (1986) 193.